High-Efficiency n-Type HP mc Silicon Solar Cells

Jan Benick, Armin Richter, Ralph Müller, Hubert Hauser, Frank Feldmann, Patricia Krenckel, Stephan Riepe, Florian Schindler, Martin C. Schubert, Martin Hermle, Andreas W. Bett, and Stefan W. Glunz

***Abstract*—Silicon solar cells featuring the highest conversion efficiencies are made from monocrystalline n-type silicon. The superior crystal quality of high-performance multicrystalline silicon (HP mc) in combination with the inherent benefits of n-type doping (higher tolerance to common impurities) should allow the fabrication of high-efficiency solar cells also on mc silicon. In this paper, we address high-efficiency n-type HP mc solar cells with diffused boron front emitter and full-area passivating rear contact (TOPCon). n-type HP mc silicon was crystallized at Fraunhofer ISE featuring a very high average lifetime in the range of 600 μs (i.e., diffusion length >800 μm) after application of all high-temperature steps necessary for cell fabrication. Using a "black silicon" front texture we have achieved a weighted reflectance of ~1% and simultaneously a very good electrical performance, i.e., J_{0e} values of ≤ 60 fA/cm^2 for a 90 Ω/sq emitter. The resulting n-type mc silicon solar cells show certified conversion efficiencies up to 21.9%, representing the current world record for mc silicon solar cells.**

***Index Terms*—High-efficiency solar cells, multicrystalline silicon, n-type silicon.**

I. Introduction

MULTICRYSTALLINE (mc) p-type silicon accounts for ~70% of the global solar cell production [1]. Though mc silicon suffers from a higher carrier recombination due to structural defects and higher concentrations of impurities, the simpler crystallization process of the mc silicon promises cost advantages over monocrystalline silicon. Whereas for industrial-type screen-printed p-type monocrystalline solar cells, efficiencies up to 22.6% [2] have been reported, for a comparably processed p-type mc solar cell, the highest certified efficiencies reported so far are 21.3% [3] and 21.6% [4]. Nevertheless, the highest efficiencies for silicon solar cells are reported for n-type silicon, where for an interdigitated back contact solar cell, a record efficiency of 26.6% was reported [5]. The superior material quality of n-type silicon is mainly due to its relative tolerance to common impurities (e.g., Fe) resulting in higher minority carrier diffusion lengths compared to p-type substrates with a similar impurity concentration [6].

For mc silicon, the change to high-performance mc silicon (HP mc) gave a significant improvement in the material quality which is mainly attributed to the strong reduction of structural defects (e.g., dislocations) in this material [7], [8]. The HP mc process combined with the inherent benefits of n-type silicon thus offers new opportunities for a low-cost, high-efficiency silicon material which might reduce the efficiency gap to monocrystalline silicon [9].

In this paper, we apply a high-efficiency solar cell fabrication process featuring a passivating rear side contact (TOPCon [10]) on high-quality n-type HP mc silicon (see Fig. 1).

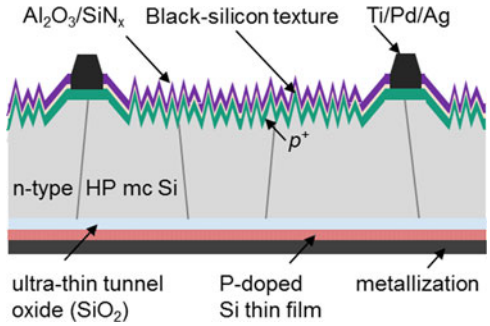

Fig. 1. Schematic of the n-type HP mc silicon solar cell.

II. n-Type HPM Silicon Quality

The n-type HP mc silicon applied in this work has been developed at Fraunhofer ISE. A research ingot of size G2 equivalent to 75 kg of pure polysilicon feedstock was crystallized by the directional solidification method with seeded growth. High purity silicon granules from a fluidized bed reactor process were placed as seed material in the bottom of a high purity fused silica crucible. As dopant material, silicon wafers enriched with 1085 ppmw phosphorus were used resulting in a resistivity profile from 1.5 Ω·cm above the remaining seed material to 0.48 Ω·cm at the ingot top. A brick with 156 mm side length was cut from the ingot center. After cropping of 15 mm at bottom and top, the brick was processed into wafers with a thickness of 195 μm by multiwire sawing with SiC slurry and structured wire. To investigate the quality of the n-type HP mc silicon, lifetime samples have been fabricated on wafers from the upper

Manuscript received March 23, 2017; revised May 22, 2017; accepted May 29, 2017. Date of publication July 19, 2017; date of current version August 18, 2017. This work was supported by the German Federal Ministry for Economic Affairs and Energy under contract number 0324034 (multiTOP). *(Corresponding author: Jan Benick.)*

J. Benick, A. Richter, H. Hauser, P. Krenckel, S. Riepe, F. Schindler, M. C. Schubert, M. Hermle, and A. W. Bett are with the Fraunhofer Institute for Solar Energy Systems, Freiburg 79110, Germany (e-mail: jan.benick@ise.fraunhofer.de; armin.richter@ise.fraunhofer.de; hubert.hauser@ise.fraunhofer.de; patricia.krenckel@ise.fraunhofer.de; stephan.riepe@ise.fraunhofer.de; florian.schindler@ise.fraunhofer.de; martin.schubert@ise.fraunhofer.de; martin.hermle@ise.fraunhofer.de; andreas.bett@ise.fraunhofer.de).

R. Müller, F. Feldmann, and S. W. Glunz are with the Fraunhofer Institute for Solar Energy Systems, Freiburg 79110, Germany, and also with the Laboratory for Photovoltaic Energy Conversion, University of Freiburg, Freiburg 79110, Germany (e-mail: ralph.mueller@ise.fraunhofer.de; frank.feldmann@ise.fraunhofer.de; stefan.glunz@ise.fraunhofer.de).

Color versions of one or more of the figures in this paper are available online at http://ieeexplore.ieee.org.

Digital Object Identifier 10.1109/JPHOTOV.2017.2714139

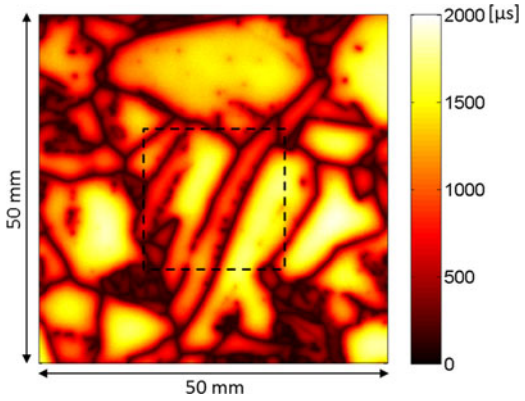

Fig. 2. Minority carrier lifetime image of a $50 \times 50\,\mathrm{mm}^2$ section of an n-type HP mc silicon wafer after high-temperature processing. The measurement was done at 0.05 sun. The dashed square ($20 \times 20\,\mathrm{mm}^2$) shows the area where on a sister wafer the best solar cell has been processed.

ingot part with a bulk resistivity of about 0.7 Ω·cm. The lifetime samples received the same high-temperature processes as used in the solar cell process sequence, i.e., boron diffusion and annealing of the TOPCon layer. After cleaning (HNO_3, followed by a HF-dip), the lifetime samples received a tube furnace boron diffusion at 890 °C with one side of the wafer being masked by a SiO_x deposited by plasma enhanced chemical vapor deposition (PECVD). Then, the boron silicate glass and the SiO_x mask were removed in HF and the high temperature step necessary for the annealing of the TOPCon layer was applied (N_2, 800 °C). As a last step, the boron emitter was removed in a wet-chemical process and the wafers were passivated by SiN_x.

To characterize the base material quality (minority carrier lifetime), photoluminescence imaging calibrated by harmonically modulated photoluminescence [11] has been performed. Exemplarily, the lifetime imaging of the middle part of one n-type HP mc silicon wafer ($50 \times 50\,\mathrm{mm}^2$, sister wafer of the best solar cell) is shown in Fig. 2. The dashed square marks the area where the best solar cells have been processed on a sister wafer. The measurement was performed at constant illumination of 0.05 sun which is representative for the maximum power point of the fabricated solar cells. The best grains show effective lifetimes >1.5 ms. However, near the grain boundaries, at the boundaries itself and at some defective areas, the lifetime is significantly reduced. Nevertheless, the average lifetime of the 50×50 mm^2 wafer section shown in Fig. 2 (square root harmonic average) is still close to 600 μs. This corresponds to a minority carrier diffusion length of more than 800 μm which is more than 4 times the cell thickness (195 μm). Thus, the applied n-type HP mc material is expected to be well suited for the fabrication of high-efficiency solar cells.

A more detailed analysis of the n-type HP mc silicon will be presented elsewhere [12].

III. TOPCon Rear Side Passivation

For the realization of the rear side of the solar cells, passivating contacts based on the approach presented by Feldmann *et al.* (TOPCon [10]) have been applied. This rear side structure consists of a wet chemically grown (HNO_3) thin tunneling oxide (∼1.2–1.4 nm) covered by a thin layer (∼15 nm) of PECVD deposited a-SiC_x:P. With this structure, we showed already in the past a very efficient passivation of mc surfaces resulting in diffusion lengths >800 μm. Details about the application of the TOPCon layer on mc silicon can be found in [9].

IV. Surface Texture

On monocrystalline silicon, pyramidal textures can be realized by anisotropic etching in alkaline solutions. This surface texture in combination with an antireflection coating enables excellent optical properties with weighted reflectances in the range of 2% against air. However, for mc silicon, this type of surface texture cannot be applied. In industrial production, acidic solutions are used for the surface texturing of mc silicon [13]. However, such surface structures do not reach the excellent optical and electrical quality of pyramidal textures. Nonetheless, first cell results with isotextured front surfaces already demonstrated the high efficiency potential of TOPCon solar cells based on n-type mc silicon substrates [9].

Alternative textures, which allow for excellent surface reflectance also on mc silicon, are honeycomb textures [14], [15] or black silicon [16], [17]. Already the 20.4% efficient mc record cell presented by Schultz *et al.* in 2004 [14] featured a honeycomb texture based on photolithography. Today several methods for the realization of honeycomb structures exist, based on nanoimprint lithography [15], inkjet [18], or laser processes [19]. The quality of such a honeycomb texture is similar to a pyramidal texture on monocrystalline silicon.

The approach which was applied in this work for the realization of the front side texture is a black silicon texture. This nanostructured surface allows for a nearly perfect coupling of the incident light. The former issue with this texture, the passivation of the nanostructured surface, was solved by an atomic layer deposition (ALD) of Al_2O_3 [20]–[23]. For the realization of the black silicon surface texture an inductively coupled plasma (ICP) process with a very low bias voltage was applied in order to keep the damage as low as possible [24]. This process was performed with an Oxford ICP133 tool using SF_6 and O_2. Note that no separate damage etch back prior surface passivation is necessary. An SEM micrograph of the resulting black silicon texture applied for the solar cells fabricated in this study is shown in Fig. 3. As can be seen, the ICP texture does not feature perfectly steep needles as known for a "classical" black silicon texture [21]. The aspect ratio of this texture is in the range of 2.

The reflectance measurement is shown in Fig. 4. Without any antireflection coating, the surface reflection weighted with the AM1.5G solar spectrum in the range from 280 to 1000 nm (R_w) is about 2.5%. To further reduce the surface reflection, an antireflection coating (ALD Al_2O_3/PECVD SiN_x) was deposited. The ALD process leads to a uniform coating of 10 nm Al_2O_3, whereas the thickness of the SiN_x layer varies between 10 and ∼100 nm due to the nonconformality of the PECVD process on the textured surface. Applying the antireflection coating reduces the weighted reflectance to ∼1%. Thus, a very effective

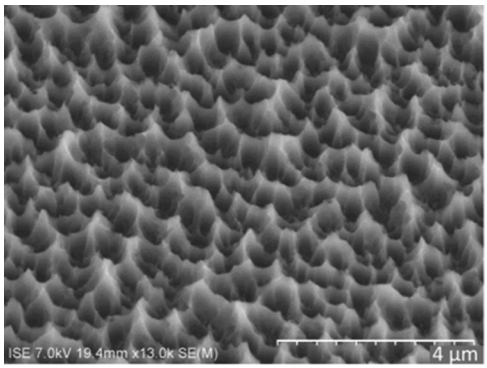

Fig. 3. SEM micrograph of the front side texture (black silicon) of the n-type HP mc solar cells.

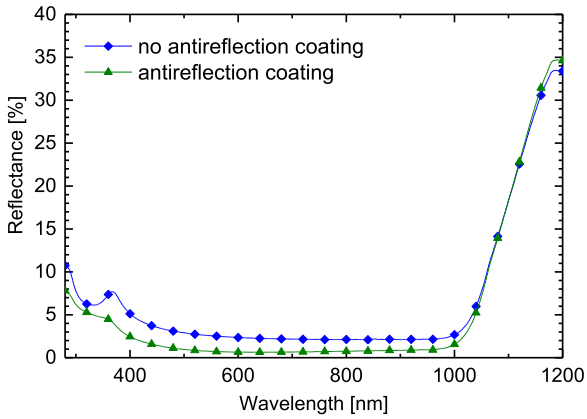

Fig. 4. Measured reflectance of the black silicon like ICP texture without and with antireflection coating.

coupling of the incident light can be reached with the applied surface texture.

In addition to good optical properties, the front side texture also needs to be compatible with emitter diffusion and surface passivation. For this reason, lifetime test samples (n-type, float-zone, 1–10 Ω cm) have been fabricated. The samples are either planar, feature a both-side random pyramids texture, or a single-side black silicon texture. All samples received a BBr_3 tube furnace boron diffusion at 890 °C (R_{sheet}: 90 Ω/sq, N_{surf} : $8 \times 10^{19}\,\mathrm{cm}^{-3}$, depth: 0.3 μm) and then were passivated by PA-ALD-deposited Al_2O_3 (10 nm) [25], [26]. The saturation current density to quantify the surface recombination was extracted from injection-dependent effective lifetime data measured using quasi steady state photoconductance (QSSPC) [27] according to the high-injection method proposed by [28] and applying the correction routines introduced by [29].

The extracted saturation current densities (for a single surface) are summarized in Table I. For the planar reference samples, a saturation current density in the range of 25 ± 5 fA/ cm^2 was measured. For both, random pyramids and black silicon texture, the saturation current density is increased to 50 ± 10 fA/ cm^2 which will still allow for high maximum open-circuit voltages >700 mV (assuming no additional recombination). Applying no surface passivation (e.g., underneath the metal contacts), the saturation current density of the applied boron emitter (calculated by EDNA [30], 25 °C) is approximately ∼1100 fA/cm^2.

TABLE I
MEASURED SATURATION CURRENT DENSITIES OF SAMPLES WITH A PLANAR, RANDOM PYRAMIDS, OR BLACK SILICON TEXTURED SURFACE

Surface	J_{0e} [fA/cm^2]
Planar	25 ± 5
Random pyramids	50 ± 10
Black silicon	50 ± 10

The surfaces feature the 90 Ω/sq boron diffusion, as applied for the fabricated solar cells and are passivated by Al_2O_3.

V. SOLAR CELLS

To investigate the excellent quality of the n-type HP mc silicon also at the device level, high-efficiency solar cells with passivating rear side contacts (TOPCon [10]) have been processed on n-type HP mc silicon (195 μm, 0.7 Ω·cm) fabricated at Fraunhofer ISE (cell structure see Fig. 1). As a reference, solar cells on float-zone silicon have been fabricated (n-type, 1 Ω·cm, 200 μm).

The processing of these n-type HP mc TOPCon solar cells starts with the definition and texturing of the active cell area (7 solar cells on each wafer, cell size 20×20 mm^2). The front side black silicon texture applied for the HP mc solar cells is realized by a plasma etching step (ICP as introduced in Section III). The FZ reference solar cells were textured in a KOH-based solution resulting in a random pyramids surface. To define the cells on every wafer, emitter windows are opened in an oxide mask (PECVD SiO_x) and the uniform boron emitter subsequently is realized by the BBr_3 tube furnace diffusion at 890 °C ($R_{\mathrm{sheet}} = 90\ \Omega/\mathrm{sq}$). After the removal of the boron silicate glass in HF, the passivating rear side contact (TOPCon [10]) is deposited and activated by an annealing step at 800 °C. Then, the front side is passivated by an Al_2O_3/SiN_x layer stack deposited via PA-ALD and PECVD, respectively. The front side contacts (area fraction ∼1.7%) are realized by photolithography and evaporation of a Ti/Pd/Ag layer stack. To ensure the electrical contact and completely activate the passivation of front and rear side, the samples received an annealing step in atomic hydrogen (remote plasma hydrogen passivation, 425 °C). For the rear side contact, a 1 μm thick Ag layer was evaporated. The final structure of the cells is shown in Fig. 1.

The measured *IV* data of the best cells are summarized in Table II. As can be seen, for the FZ reference cells, high conversion efficiencies up to 23.3% could be reached with V_{oc} of 684 mV, J_{sc} of 41.5 mA/cm^2, and FF of 82.2%. The comparison of the measured *IV* data with three-dimensional total area Quokka [31] device simulations (688.2 mV, 41.6 mA/cm^2, 82.5%) using experimentally determined input parameters (e.g., $J_{0e,\mathrm{total}} = 70$ fA/ cm^2, $J_{0,\mathrm{TOPCon}} = 7$ fA/ cm^2, measured reflection, including cell perimeter) reveals that almost the full potential of the applied cell structure was exploited and no significant process-related issues occurred during cell fabrication.

TABLE II
IV MEASUREMENTS (AM1.5 g, 100 MW/CM^2, 25 °C) OF THE BEST CELLS OF EACH GROUP (N-TYPE FZ WITH RANDOM PYRAMIDS TEXTURE AND N-TYPE HP MC SILICON EITHER WITH PLANAR OR BLACK SILICON TEXTURED SURFACE)

V_{oc} [mV]	J_{sc} [mA/cm^2]	*FF* [%]	*pFF* [%]	η [%]
n-type FZ, random pyramids				
683.9	41.5	82.2	84.1	23.3
n-type HP mc, planar surface				
676.1	37.3	79.5	81.7	20.1
n-type HP mc, black silicon texture				
672.6	40.8	79.7	81.6	21.9*

*Certified measurement by Fraunhofer ISE CalLab (4 cm^2, aperture area).

For the n-type HP mc silicon solar cells, very high conversion efficiencies up to 21.9% have also been reached with V_{oc} of 673 mV, J_{sc} of 40.8 mA/ cm^2, and FF of 79.7%. This represents the highest efficiency ever reached for an mc silicon solar cell. However, there is still a significant gap to the monocrystalline reference solar cells. Regarding the open-circuit voltage, the mc solar cells show values which are about 10 mV lower than those of the FZ references. Based on J_{0e} measured for the boron-doped black silicon texture, this difference cannot be attributed to a difference in the emitter and surface recombination. This is also confirmed by the n-type HP mc solar cells featuring a planar surface. For these cells, only a slightly higher V_{oc} of 676 mV was measured, which is still below the voltage of the FZ references, although the respective J_{0e} is only about half the J_{0e} of the random pyramids textured surface. The small difference in V_{oc} for the solar cells featuring a planar surface and the black silicon texture also confirms that the black silicon surface with the 90 Ω/sq emitter boron-doped emitter is very effectively passivated as also observed on the lifetime test structures (see Table I).

The fill factor of the n-type HP mc silicon solar cells (planar as well as black silicon textured surface) with values in the range of 79.5% is relatively high. However, the applied cell structure allows for significantly higher values, as is shown by about 2.5%$_{abs}$ higher fill factors of the FZ references. As the pseudo-FF shows the same difference (∼81.5% for the HP mc, ∼84% for the FZ), the lower FF of the mc solar cells cannot be attributed to series resistance effects (R_{series} of best cell ∼0.4 Ω·cm^2). As the parallel resistance with >4 kΩ·cm^2 is sufficiently high, the reduced pseudo-FF most probably is either directly related to the quality of the base material, e.g., recombination at maximum power point, or to effects related to the mc nature of the material.

The J_{sc} of 40.8 mA/ cm^2 is very high for an mc silicon solar cell and shows that the black silicon texture leads to an effective reduction of the surface reflection. Nevertheless, also in J_{sc}, a difference to the FZ reference solar cell can be observed which shows J_{sc} of 41.5 mA/ cm^2. The measured reflectance curves of the different solar cells (see Fig. 5) shows that the reflectance curve of the black silicon textured HP mc silicon solar cell especially in the short wavelength range is actually significantly

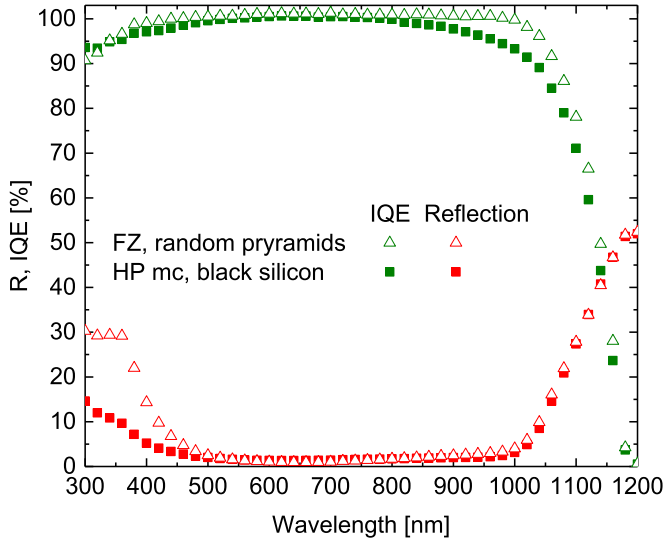

Fig. 5. Quantum efficiency and reflection curves of the n-type HP mc solar cell with a black silicon surface texture as well as of the n-type FZ reference with a random pyramids texture.

better than that of the pyramidal texture of the reference solar cell. In the long wavelength range, both textures show identical reflectance curves, showing that the light trapping capabilities of the black silicon and the random pyramids are comparable.

Regarding the internal quantum efficiency (see Fig. 5), however, a significant difference in the long wavelength range >800 nm can be observed. Whereas the FZ reference solar cell shows an internal quantum efficiency of 100% up to a wavelength of 1000 nm, the quantum efficiency of the HP mc silicon solar cell at 1000 nm is reduced to ∼90%. As both cells feature the same rear side structure (TOPCon), this difference is also most probably related to the base material.

Thus, despite the fact that excellent conversion efficiencies could be achieved on the applied n-type HP mc silicon, it has to be stated that limitations due to the material still occur. However, the difference of the low cost HP mc silicon to the highest quality FZ silicon could be significantly reduced [9]. The origin of the remaining material limitations will be investigated in more detail in future work which may allow a further optimization of the quality of the already very good mc silicon material.

VI. SUMMARY

High-efficiency solar cells with diffused boron front emitter and full-area passivating rear contact (TOPCon) on n-type HP mc silicon (fabricated at Fraunhofer ISE) have been developed in this work. Lifetime measurements after high-temperature processing revealed that a high average lifetime of ∼600 μs (diffusion length >800 μm) can be achieved without a dedicated P-gettering step. To ensure optimum coupling of the incident light, a black silicon texture was developed, reducing the weighted reflectance to 1%. For a 90 Ω/sq boron emitter passivated by Al_2O_3, J_{0e} values < 60 fA/cm^2 were achieved for this surface. High-efficiency solar cells fabricated from the n-type HP mc silicon resulted in a record efficiency of 21.9%.

ACKNOWLEDGMENT

The authors would like to thank A. Leimenstoll, F. Schätzle, S. Seitz, A. Seiler, C. Harmel, R. van der Vossen, and E. Schäffer for their support with processing and measurements.

REFERENCES

[1] Photovoltaics Report - Fraunhofer ISE. [Online]. Available: https://www.ise.fraunhofer.de/de/daten-zu-erneuerbaren-energien.html. Accessed on: Mar. 14, 2017.

[2] *Press Releases | Trina Solar*. [Online]. Available: http://phx.corporate-ir.net/phoenix.zhtml?c = 206405&p = irol-newsArticle&ID = 2230468. Accessed on: Feb. 24, 2017.

[3] W. Deng *et al.*, "Development of high-efficiency industrial p-type multicrystalline PERC solar cells with efficiency greater than 21%," *Energy Procedia*, vol. 92, pp. 721–729, 2016.

[4] P. Zheng *et al.*, "21.63% industrial screen-printed multicrystalline Si solar cell," *Phys. Status Solidi RRL*, vol. 11, 2017, Art. no. 1600453.

[5] K. Yoshikawa *et al.*, "Silicon heterojunction solar cell with interdigitated back contacts for a photoconversion efficiency over 26%," *Nature Energy*, vol. 2, 2017, Art. no. 17032.

[6] D. Macdonald and L. J. Geerligs, "Recombination activity of interstitial iron and other transition metal point defects in p-and n-type crystalline silicon," *Appl. Phys. Lett.*, vol. 85, no. 18, pp. 4061–4063, 2004.

[7] Y. M. Yang *et al.*, "Development of high-performance multicrystalline silicon for photovoltaic industry," *Prog. Photovolt.: Res. Appl.*, vol. 23, no. 3, pp. 340–351, 2015.

[8] S. Castellanos *et al.*, "High-performance and traditional multicrystalline silicon: Comparing gettering responses and lifetime-limiting defects," *IEEE J. Photovolt.*, vol. 6, no. 3, pp. 632–640, May 2016.

[9] F. Schindler *et al.*, "High-efficiency multicrystalline silicon solar cells: Potential of n-type doping," *IEEE J. Photovolt.*, vol. 5, no. 6, pp. 1571–1579, Nov. 2015.

[10] F. Feldmann, M. Bivour, C. Reichel, M. Hermle, and S. W. Glunz, "Passivated rear contacts for high-efficiency n-type Si solar cells providing high interface passivation quality and excellent transport characteristics," *Sol. Energy Mater. Sol. Cells*, vol. 120, pp. 270–274, 2014.

[11] J. A. Giesecke, M. C. Schubert, B. Michl, F. Schindler, and W. Warta, "Minority carrier lifetime imaging of silicon wafers calibrated by quasi-steady-state photoluminescence," *Sol. Energy Mater. Sol. Cells*, vol. 95, no. 3, pp. 1011–1018, 2011.

[12] F. Schindler *et al.*, "Multicrystalline silicon for solar cell efficiencies exceeding 22%," *Sol. Energy Mater. Sol. Cells*, vol. 171, pp. 180–186, 2017.

[13] A. Hauser *et al.*, "A simplified process for isotropic texturing of mc-Si," in *Proc. 3rd World Conf. Photovolt. Energy Convers.*, 2003, pp. 1447–1450.

[14] O. Schultz, S. W. Glunz, and G. P. Willeke, "Multicrystalline silicon solar cells exceeding 20% efficiency," *Prog. Photovolt.: Res. Appl.*, vol. 12, no. 7, pp. 553–558, 2004.

[15] H. Hauser *et al.*, "Honeycomb texturing of silicon via nanoimprint lithography for solar cell applications," *IEEE J. Photovolt.*, vol. 2, no. 2, pp. 114–122, Apr. 2012.

[16] J. Oh, H.-C. Yuan, and H. M. Branz, "An 18.2%-efficient black-silicon solar cell achieved through control of carrier recombination in nanostructures," *Nature Nanotechnol.*, vol. 7, no. 11, pp. 743–748, 2012.

[17] P. Repo *et al.*, "N-type black silicon solar cells," *Energy Procedia*, vol. 38, pp. 866–871, 2013.

[18] N. Borojevic, A. Lennon, and S. Wenham, "Inkjet texturing for multicrystalline silicon solar cells," in *Proc. 24th Eur. Photovolt. Sol. Energy Conf.*, 2009, pp. 1975–1978.

[19] D. Niinobe *et al.*, "Honeycomb structured multi-crystalline silicon solar cells with 18.6% efficiency via industrially applicable laser-process," in *Proc. 23rd Eur. Photovolt. Sol. Energy Conf. Exhib.*, 2008, pp. 1824–1828.

[20] M. Algasinger *et al.*, "Improved black silicon for photovoltaic applications," *Adv. Energy Mater.*, vol. 3, no. 8, pp. 1068–1074, 2013.

[21] P. Repo *et al.*, "Effective passivation of black silicon surfaces by atomic layer deposition," *IEEE J. Photovolt.*, vol. 3, no. 1, pp. 90–94, Jan. 2013.

[22] P. Repo *et al.*, "Passivation of black silicon boron emitters with atomic layer deposited aluminum oxide," *Phys. Status Solidi RRL*, vol. 7, no. 11, pp. 950–954, 2013.

[23] M. Otto *et al.*, "Extremely low surface recombination velocities in black silicon passivated by atomic layer deposition," *Appl. Phys. Lett.*, vol. 100, no. 19, 2012, Art. no. 191603.

[24] J. Hirsch, M. Gaudig, N. Bernhard, and D. Lausch, "Optoelectronic properties of Black-Silicon generated through inductively coupled plasma (ICP) processing for crystalline silicon solar cells," *Appl. Surf. Sci.*, vol. 374, pp. 252–256, 2016.

[25] B. Hoex *et al.*, "Excellent passivation of highly doped p-type Si surfaces by the negative-charge-dielectric Al2O3," *Appl. Phys. Lett.*, vol. 91, no. 11, 2007, Art. no. 112107.

[26] A. Richter, J. Benick, and M. Hermle, "Boron emitter passivation with Al2O3 and Al2O3/SiNx stacks using ALD Al2O3," *IEEE J. Photovolt.*, vol. 3, no. 1, pp. 236–245, Jan. 2013.

[27] R. A. Sinton and A. Cuevas, "Contactless determination of current–voltage characteristics and minority-carrier lifetimes in semiconductors from quasi-steady-state photoconductance data," *Appl. Phys. Lett.*, vol. 69, no. 17, pp. 2510–2512, 1996.

[28] D. E. Kane and R. M. Swanson, "Measurement of the emitter saturation current by a contactless photoconductivity decay method," in *Proc. 18th IEEE Photovolt. Spec. Conf.*, 1985, pp. 374–379.

[29] A. Kimmerle, J. Greulich, and A. Wolf, "Carrier-diffusion corrected J0-analysis of charge carrier lifetime measurements for increased consistency," *Sol. Energy Mater. Sol. Cells*, vol. 142, pp. 116–122, 2015.

[30] K. R. McIntosh and P. P. Altermatt, "A freeware 1D emitter model for silicon solar cells," in *Proc. 35th IEEE Photovolt. Spec. Conf.*, 2010, pp. 002188–002193.

[31] A. Fell, "A free and fast three-dimensional/two-dimensional solar cell simulator featuring conductive boundary and quasi-neutrality approximations," *IEEE Trans. Electron Devices*, vol. 60, no. 2, pp. 733–738, Feb. 2013.

Authors' photographs and biographies not available at the time of publication.